







Cardiomyocytes from female compared to male mice have larger ryanodine receptor clusters and higher calcium spark frequency

Martin Laasmaa^{1,2,3} , Jelena Branovets¹ , Jekaterina Stolova¹, Xin Shen^{2,3} , Triinu Rätsepso¹, Mihkel Jaan Balodis¹, Cärolin Grahv¹, Eliise Hendrikson¹, William Edward Louch^{2,3} , Rikke Birkedal¹  and Marko Vendelin¹ 

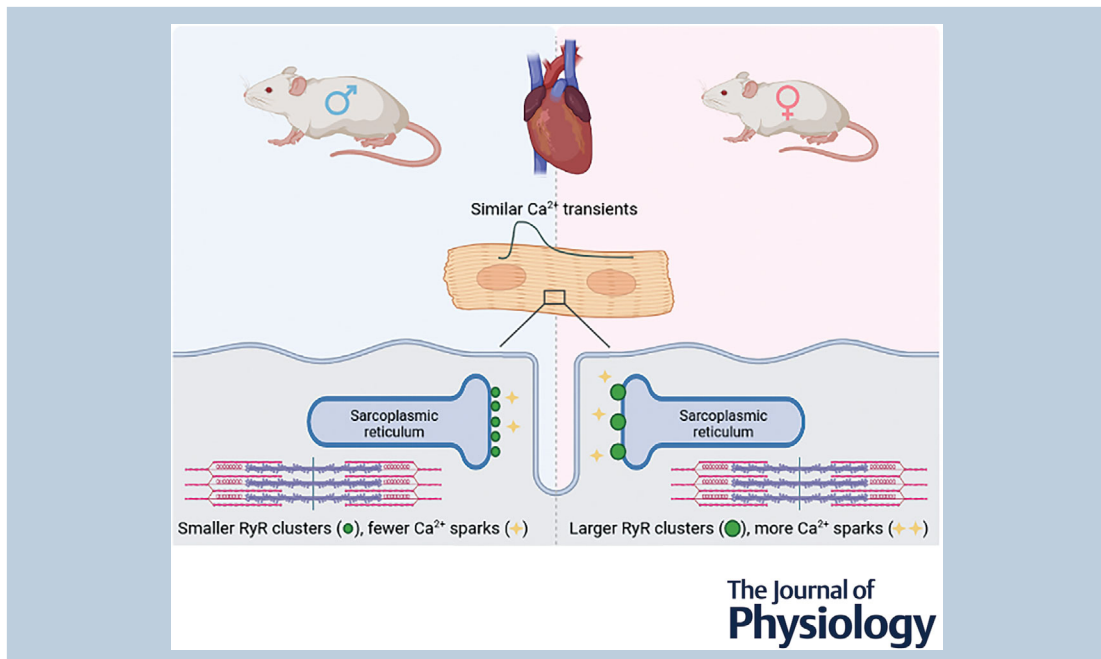
¹Laboratory of Systems Biology, Department of Cybernetics, Tallinn University of Technology, Tallinn, Estonia

²Institute for Experimental Medical Research, University of Oslo, Oslo, Norway

³K.G. Jebsen Centre for Cardiac Research, University of Oslo, Oslo, Norway

Handling Editors: Bjorn Knollmann & Michael Shattock

The peer review history is available in the Supporting Information section of this article (<https://doi.org/10.1113/JP284515#support-information-section>).



Martin Laasmaa obtained his doctoral degree in physics at Tallinn University of Technology (TalTech) in Estonia under the tutelage of Prof. Marko Vendelin, after which he joined Prof. William Louch's group in Norway at the Institute for Experimental Medical Research in Oslo as a postdoctoral fellow. After his postdoctoral studies, he moved back to TalTech and is currently an Assistant Professor at the Institute of Cybernetics at TalTech. His main focus is understanding calcium handling in cardiomyocytes in health and disease by combing functional and structural studies (as well as mathematical modelling). **Jelena Branovets** obtained her doctoral degree in gene technology at Tallinn University of Technology (TalTech) in Estonia. She then continued to work as a Researcher at the Laboratory of Systems Biology at the Institute of Cybernetics at TalTech. Her main research interests are associated with the physiology of the heart. She is interested in regulation of energy production and how it is linked to cardiomyocyte morphology and excitation–contraction coupling.



M. Laasmaa and J. Branovets contributed equally to this work.

Abstract Sex differences in cardiac physiology are receiving increased attention as it has become clear that men and women have different aetiologies of cardiac disease and require different treatments. There are experimental data suggesting that male cardiomyocytes exhibit larger Ca^{2+} transients due to larger Ca^{2+} sparks and a higher excitation–contraction coupling gain; in addition, they exhibit a larger response to adrenergic stimulation with isoprenaline (ISO). Here, we studied whether there are sex differences relating to structural organization of the transverse tubular network and ryanodine receptors (RyRs). Surprisingly, we found that female cardiomyocytes exhibited a higher spark frequency in a range of spark magnitudes. While overall RyR expression and phosphorylation were the same, female cardiomyocytes had larger but fewer RyR clusters. The density of transverse t-tubules was the same, but male cardiomyocytes had more longitudinal t-tubules. The Ca^{2+} transients were similar in male and female cardiomyocytes under control conditions and in the presence of ISO. The synchrony of the Ca^{2+} transients was similar between sexes as well. Overall, our data suggest subtle sex differences in the Ca^{2+} influx and efflux pathways and their response to ISO, but these differences are balanced, resulting in similar Ca^{2+} transients in field-stimulated male and female cardiomyocytes. The higher spark frequency in female cardiomyocytes is related to the organization of RyRs into larger, but fewer clusters.

(Received 8 February 2023; accepted after revision 7 July 2023; first published online 10 August 2023)

Corresponding author M. Vendelin: Laboratory of Systems Biology, Department of Cybernetics, School of Science, Tallinn University of Technology Akadeemia 21, 12618 Tallinn, Estonia. Email: markov@sysbio.ioc.ee

Abstract Figure Legend Despite subtle sex differences in cardiomyocyte structure and calcium fluxes, the differences are balanced, leading to similar calcium transients in cardiomyocytes from male and female mice.

Key points

- During a heartbeat, the force of contraction depends on the amplitude of the calcium transient, which in turn depends on the amount of calcium released as calcium sparks through ryanodine receptors in the sarcoplasmic reticulum.
- Previous studies suggest that cardiomyocytes from male compared to female mice exhibit larger calcium sparks, larger sarcoplasmic reticulum calcium release and greater response to adrenergic stimulation triggering a fight-or-flight response.
- In contrast, we show that cardiomyocytes from female mice have a higher spark frequency during adrenergic stimulation and similar spark morphology.
- The higher spark frequency is related to the organization of ryanodine receptors into fewer, but larger clusters in female compared to male mouse cardiomyocytes.
- Despite subtle sex differences in cardiomyocyte structure and calcium fluxes, the differences are balanced, leading to similar calcium transients in cardiomyocytes from male and female mice.

Introduction

There are many differences between females and males regarding heart anatomy and function. In addition to heart size, there are differences in heart rate, electrophysiology and response to stress (Prajapati et al., 2022; St. Pierre et al., 2022). The differences in normal function extend to differences in cardiac diseases and ageing (Beale et al., 2018; Keller & Howlett, 2016; Odening et al., 2019; Regitz-Zagrosek & Kararigas, 2016; Yusifov et al., 2022). For example, adrenergic activation had sex- and age-dependent effects on cardiac structure and function (Yusifov et al., 2021). From a clinical perspective, women

and men are prone to different types of ischaemic heart diseases at different ages, and the clinical outcome also depends on sex (Regitz-Zagrosek & Kararigas, 2016). However, the mechanisms behind these differences are not fully understood and require further study (Prajapati et al., 2022; St. Pierre et al., 2022; Yusifov et al., 2022).

Sex differences are observed from organ to cellular and sub-cellular levels (Trexler et al., 2017) and in all types of cells in the heart (Walker et al., 2021). In cardiomyocytes, sex differences have been demonstrated in contractility, excitation–contraction coupling and response to β -adrenergic stimulation (Parks & Howlett, 2013). Experimental data is frequently summarized as

cardiomyocytes from males exhibiting greater contractility than females with Ca^{2+} transients following a similar pattern, i.e. males have larger transients and greater response to β -adrenergic stimulation than females (Parks & Howlett, 2013; Prajapati et al., 2022). Differences in Ca^{2+} transients have been associated with male cardiomyocytes having larger Ca^{2+} sparks – elementary Ca^{2+} release events – and higher excitation–contraction coupling gain, i.e. a greater sarcoplasmic reticulum (SR) Ca^{2+} release per Ca^{2+} -influx through the L-type Ca^{2+} channel (Farrell et al., 2010; Parks et al., 2014).

Ca^{2+} sparks and transients are influenced by structural factors such as ryanodine receptor (RyR) clustering and organization of the transverse tubular (t-tubular) network. These play a vital role in Ca^{2+} handling and are impacted in disease (Cheng & Lederer, 2008; Frisk et al., 2016; Kolstad et al., 2018; Louch et al., 2006). To the best of our knowledge, the structural organization of neither RyRs on the SR membrane nor the t-tubular network has been compared in female and male cardiomyocytes. Here, we address this knowledge gap.

The aim of this work was to determine whether, in healthy cardiomyocytes, there are any sex differences in the arrangement of RyRs and the t-tubular network in cardiomyocytes. These structural characteristics were complemented with functional recordings of Ca^{2+} sparks and Ca^{2+} transients. The latter also allowed us to determine the synchrony of Ca^{2+} release. As a part of the functional studies, we stimulated cardiomyocytes in the absence or presence of isoprenaline to test whether the response to β -adrenergic stimulation is different between sexes. Lastly, we performed western blot experiments to determine the overall RyR expression as well as its phosphorylation on Ser2808 and Ser2814, as this may influence the localization and function of RyR clusters (Shen et al., 2022).

Methods

Ethical approval

All animal procedures were carried out according to the guidelines of Directive 2010/63/EU of the European Parliament on the protection of animals used for scientific purposes and had been approved by the Project Authorisation Committee for Animal Experiments in the Estonian Ministry of Rural Affairs.

Animals

For the experiments, arginine:glycine amidinotransferase (AGAT) and guanidinoacetate methyltransferase (GAMT) wild-type mice were used (Choe et al., 2013; Schmidt et al., 2004). The animals were back-crossed for more than 10 generations with C57BL/6J OlaHsd

(Envigo). They were bred and kept at our local animal facility with free access to water and food (V1534-000 R/M-H complete maintenance diet for rats and mice; Ssniff Spezialdiäten GmbH, Soest, Germany) at an ambient temperature of 22–23°C, and a 12:12-h light–dark cycle. These animals were used as a part of a larger study on creatine deficiency and its impact on cardiac function. The female animals were chosen at random stages of their oestrous cycle.

Genotyping

AGAT and GAMT mice were genotyped as in Branovets et al. (2013, 2021) and Laasmaa et al. (2021).

Cardiomyocyte isolation

Mice were anaesthetized with a ketamine/dexmedetomidine mixture (150 and 0.5 mg kg⁻¹, respectively) and received an injection of 250 U of heparin to prevent blood coagulation. When the toe-pinch reflex was absent, the animal was euthanized by cervical dislocation. The heart was immediately excised and transferred to an ice-cold wash solution. Cardiomyocytes were isolated as in Branovets et al. (2013, 2021) and Laasmaa et al. (2021).

Detection and analysis of calcium transients and sparks

Ca^{2+} sparks and transients were detected according to a previously described protocol (Laasmaa et al., 2019). Freshly isolated cardiomyocytes were loaded in the presence of 5 μM fluo-4 AM (Thermo Fisher Scientific, Waltham, MA, USA) for 20 min in Tyrode solution containing (in mM): 150 NaCl, 5.4 KCl, 0.33 NaH₂PO₄, 1 MgCl₂, 1.13 CaCl₂, 10 glucose, and 10 HEPES (pH was adjusted to 7.4 with NaOH). After loading the cells with the Ca^{2+} sensitive dye, 100 μl of cell suspension was placed in a measuring chamber RC-21BRFS (Warner Instruments, Hamden, CT, USA), and 100 μl of Tyrode with or without 100 nM isoprenaline (ISO) was added, corresponding to conditions with or without β -adrenergic stimulation, respectively.

For experiments, rod-shaped cardiomyocytes with clear striations that responded to each stimulation pulse were chosen for imaging Ca^{2+} transient and sparks. Before starting linescan imaging, the cardiomyocyte was field-stimulated for about 5 min at 21°C with square pulses (width 10 ms, height 10 V) at 1 Hz using Stimulator C Type 224 (Harvard Apparatus, Holliston, MA, USA) connected to the imaging chamber with platinum wires. After starting the acquisition, transients were recorded for 5–15 s, after which sparks were recorded for about 100 s.

After each measurement, cells were replaced with freshly loaded cells.

Confocal images were acquired using a Zeiss LSM510 Duo confocal microscope (Zeiss Microscopy, Jena, Germany) with a $\times 63$ water-immersion objective (1.2 NA). The signal was obtained via a single high-voltage PMT using 8-bit mode; the pinhole was set to one Airy disk. Fluo-4 was excited with a 488 nm Argon laser (0.8% of the power), and after passing 488 nm dichroic, the fluorescence was recorded through a long-pass 505 nm filter. Linescans were performed unidirectionally, and *xt* images were made to cover a line of $\sim 70 \mu\text{m}$ (512 pixels, $0.14 \mu\text{m}$ pixel size) along the cell, avoiding nuclei. In total, 70,000 lines 1.53 ms apart were acquired. For background estimation, a single 2D image of each cell with the surrounding background was recorded after linescans with the same imaging configuration.

Ca^{2+} sparks were detected and analysed using default parameters with IOC BIO Sparks open-source software (Laasmaa et al., 2019). The background intensity from the separately recorded image was determined using ImageJ. Ca^{2+} transients were analysed by IOC BIO Kinetics open-source software after manually marking each Ca^{2+} transient (Vendelin et al., 2020). In this analysis, Ca^{2+} transients were fitted by monotonic cubic interpolation, and transient properties, such as amplitude, duration at half-maximum and time-moments at which transient reached half-maximum values were determined.

For further statistical analysis of calcium sparks and transients amplitude, decay time, full width at half-maximum and full duration at half-maximum were used.

Dyssynchrony index calculation

The dyssynchrony index was calculated similarly to Louch et al. (2006). In short, *xt* scan images acquired for Ca^{2+} transients and spark determination (see above) were split into smaller sections along the *x*-axis, 16 pixels per section. The signal in each section was averaged and analysed as Ca^{2+} transients above. Time-moments at which local Ca^{2+} transients reached half-maximum at the beginning of the transient (systolic), and end of the transient (diastolic) were found and stored in the central database. The dyssynchrony index was calculated as a logarithm of standard deviation of the time-moments corresponding to the systolic or diastolic phase for each transient separately. Next, the dyssynchrony index for an experiment was found as an average index of all transients measured in the experiment, usually 5–15.

Detecting t-tubular network

Freshly isolated cells were loaded with CellMask Green Plasma Membrane Stain (Thermo Fisher Scientific, C37608) at 1:1000 dilution in a solution containing

(in mM): 110 sucrose, 60 potassium lactobionic acid, 3 KH_2PO_4 , MgCl_2 , 20 HEPES, 20 taurine, 0.5 EGTA, 0.5 dithiothreitol (pH was adjusted to 7.1 with KOH). After incubation for 20 min at room temperature and sedimentation of the cells, the supernatant was removed and replaced with a fresh solution. A volume of 100–150 μl of the cell suspension was added into the chamber of a flexiPERM micro 12 reusable silicone cell culture chamber (Sarstedt AG & Co. KG, Nümbrecht, Germany) attached to a coverslip. Imaging was performed using either the Zeiss LSM 510 Duo or the Zeiss LSM 900 system with a $\times 63$ water-immersion objective (1.2 NA). CellMask was excited with a 488 nm laser. In the case of the Zeiss LSM 900, the emission in the range of 495–700 nm was collected by a gallium arsenide phosphide photomultiplier tube using the 16-bit mode. When the Zeiss LSM 510 Duo was used, emission was recorded through a 505-nm long-pass filter by a high-voltage single photomultiplier tube using 12-bit mode.

The t-tubular network was detected and analysed using Ilastik (Berg et al., 2019) and custom post-processing scripts from the confocal microscopy images. All images were stored and processed using a local OMERO server (Allan et al., 2012). First, a neural network was trained in Ilastik to classify pixels belonging to t-tubules or background. Care was taken to mark as t-tubules only the pixels close to the centre of a t-tubule to obtain as thin a representation of t-tubules as possible. Second, in all analysed images, a region corresponding to the intracellular space excluding nuclei and sarcolemma was marked in OMERO. Third, with the training ready and intracellular space marked in OMERO, we processed all images using the custom script to detect t-tubules and store the corresponding skeleton in OMERO as a region of interest. In the script, Ilastik classification was loaded, and pixels classified as belonging to the t-tubule network were dilated by one pixel. After that, connected regions were evaluated for size, and regions smaller than 16 pixels were excluded from further analysis. The remaining regions were skeletonized. The skeleton was analysed to remove small edges (smaller than 5 pixels), with the remaining skeleton saved as a region of interest in OMERO. These image manipulations were performed using packages scikit-image (Walt et al., 2014) and sknw of ImagePy (Wang et al., 2018).

With t-tubules detected and stored in OMERO, we determined the overall t-tubule network length per intracellular area. The network orientation was described by calculating the overall length of all network segments in that orientation (within a given range of angles, see Results) per unit intracellular area. The Minkowski–Bouligand fractal dimension was determined to describe branching patterns of the network.

Developed scripts are released open-source and available at <https://gitlab.com/iocbio/ttubules>.

Super-resolution imaging and image analysis

Fixed cardiomyocytes were placed on poly-L-lysine (Sigma-Aldrich, Merck KGaA, Darmstadt, Germany, P8920) coated coverslips (MatTek, P35G-0.170-14-C) and left to sediment for 30 min. Next, the supernatant was removed, and cells were permeabilized with the addition of 0.5% Triton X-100 in Dulbecco's phosphate-buffered saline (BioWhittaker Inc., Walkersville, MD, USA, cat. no. 4387) for 10 min. After permeabilization, cells were washed three times with phosphate buffered saline (PBS; 5 min between each wash) and blocked using Image-iT™ FX Signal Enhancer (Thermo Fisher Scientific, I36933) for 30 min at room temperature. Cells were immunolabelled with primary anti-RyR antibody (ThermoFisher Scientific, MA3-916) at 1:100 dilution in a low blocking buffer (2.5% normal goat serum in PBS) overnight at 4°C. The following day, cells were washed three times with PBS, after which a secondary antibody (goat anti-mouse IgG Alexa Fluor Plus 647, ThermoFisher Scientific, A32728) was added at 1:100 dilution in the low blocking buffer and incubated at room temperature for 1 h. Finally, cells were washed three times with PBS, and an imaging buffer containing 20% VectaShield (Vector Laboratories, Newark, CA, USA, H-1000) diluted in Tris-glycerol (5% v/v 1 M Tris pH 8 in glycerol, Sigma-Aldrich, Merck KGaA, Darmstadt, Germany) was added before imaging. This composition has been previously shown to produce comparable, if not superior, quality dSTORM images compared with conventional oxygen scavenging-dependent systems (Olivier et al., 2013).

Imaging was carried out using the Zeiss ELYRA/LSM 710 system equipped with a Zeiss α Plan-Apochromat 63 \times 1.46 NA objective (Zeiss Microscopy, 420780-9970-000). A 642 nm laser illumination at 300 W mm⁻² was used for excitation. For 3D imaging, the excitation beam was configured in a highly inclined and laminated optical sheet (HiLo) utilizing phase ramp imaging localization microscopy (PRILM) technology (Baddeley et al., 2011). Emission >655 nm was collected with an iXon 897 back-thinned EMCCD camera (Andor Technology, Belfast, UK), where EMCCD gain was set to 100, the frame exposure time to 40 ms, and 15,000 frames were acquired per cell. Throughout image acquisition, a piezo-operated Definite Focus system was employed to autocorrect for axial drift.

The 'PALM Processing' module in the ZEN Black software (Zeiss Microscopy) was used to reconstruct dSTORM data. In short, an 11-pixel circular mask with a signal-to-background noise ratio of 6 was used to detect individual single-fluorophore blinks. For mapping blinks to 3D space, an experimental 3D point spread function with an axial range of 4 μ m was acquired using 100 nm fluorescent beads (Thermo Fisher Scientific,

T7279). The drift correction was performed using a 5-segment piece-wise linear function. Events from only the central 600 nm of the 4 μ m stack were included for further analysis to minimize the inclusion of clusters with larger localization errors (Baddeley et al., 2011). The *x*, *y* and *z* coordinates of each localization event were saved in a comma-separated value format.

Custom Python scripts were used to estimate RyR cluster, Ca²⁺ release unit (CRU) sizes, count and density per imaging volume, the nearest neighbour distance between RyR clusters and rendering point data. Briefly, based on the point data 3D histogram was created with a bin size of 30 nm in the lateral and axial directions. The image was then convolved with a Gaussian filter whose width corresponded to single event lateral and axial precision values and thresholded image using the thresholding Otsu method. This resulted in a binary image where each voxel contained no more than a single RyR. From the binary image, RyR clusters were determined as areas where the non-zero pixels were side-by-side. RyR clusters with edges localized within 100 nm were assigned to the same CRU (Sobie et al., 2006).

Western blot analysis

Phospholamban, phospho-phospholamban Ser-16 and phospho-phospholamban Thr-17. Eight micrograms (phospho-phospholamban (pPLB) Thr-17) or 10 μ g (phospholamban (PLB) and pPLB Ser-16) of protein was preheated at 95°C for 5 min and loaded onto SDS-PAGE gels (4% stacking gel, 15% separating gel), which were run at 60 V for 35 min, followed by 120 V for 50–55 min in a Mini-PROTEAN Tetra System using a PowerPac HC power supply (Bio-Rad Laboratories, Hercules, CA, USA). The separated proteins were transferred using Trans-Blot Turbo Transfer System (Bio-Rad Laboratories) onto a 0.2 μ m polyvinylidene difluoride membrane for 5 min following the Bio-Rad low molecular mass protocol (2.5 A, up to 25 V).

RyR, phospho-RyR Ser-2808 and phospho-RyR Ser-2814. Thirty microgram (RyR and phospho (p)RyR Ser-2808) or 50 μ g (pRyR Ser-2814) of protein was preheated at 37°C for 10 min (RyR and pRyR Ser-2808) or 15 min (pRyR Ser-2814) and loaded onto SDS-PAGE Mini-PROTEAN TGX precasted gels (4–15%, Bio-Rad Laboratories), which were run at 120 V for 1 h in a Mini-PROTEAN Tetra System using a PowerPac HC power supply (Bio-Rad Laboratories). The separated proteins were transferred onto a 0.45 μ m PVDF membrane for 1 h on ice at 0.35 A (RyR and pRyR Ser-2808) or using Trans-Blot Turbo Transfer System (Bio-Rad Laboratories) for 10 min following Bio-Rad high MW protocol (1.3 A, up to 25 V; pRyR Ser-2814).

After transfer, the membranes were incubated in Tris-buffered saline with 0.1% Tween-20 (TBST) containing various reagents. They were blocked for 1 h with 5% non-fat milk or 3% BSA (pRyR Ser-2814) and then incubated with primary antibody in TBST containing 5% BSA or no BSA (pRyR Ser-2814) overnight at 4°C. The next day, the membranes were incubated with secondary antibody in 5% BSA or 3% BSA (pRyR Ser-2814) for 1 h at room temperature. Between each step, the membranes were washed three times for 7–10 min in TBST. After the final wash, the antibody labelling was detected with the Bio-Rad Clarity Western ECL substrate, imaged in an Image Quant LAS 400 imager (GE Healthcare, Chicago, IL, USA). The following primary antibodies were used: PLB (Abcam, Cambridge, United Kingdom, ab86930, RRID AB_1 952 347, dilution 1:1000); PLB-phospho-Ser16 (Abcam, Cambridge, United Kingdom, ab15000, RRID AB_301 562, dilution 1:1000); PLB-phospho-Thr17 (Badrilla A010-13AP, RRID AB_2 617 048, dilution 1:1000); RyR2 (Thermo Fisher Scientific PA5-87 416, RRID AB_2 804 131, dilution 1:2000); RyR2-phospho-S2808 (Abcam, Cambridge, United Kingdom, ab59225, RRID AB_946 327, dilution 1:2000), RyR2-phospho-S2814 (Badrilla A010-31, RRID:AB_2 617 055, dilution 1:1000). Anti-glyceraldehyde 3-phosphate dehydrogenase (GAPDH) (Cell Signaling Technology, Danvers, MA, USA, 2118, RRID AB_561 053) was used to assess the expression of GAPDH, a commonly used housekeeping protein. When assessing PLB relative to GAPDH, the anti-GAPDH dilution was 1:6000, when assessing RyR and pRyR Ser-2808 relative to GAPDH, the anti-GAPDH dilution was 1:8000, and when assessing pRyR Ser-2814 relative to GAPDH, the anti-GAPDH dilution was 1:10,000. The secondary antibody was a horseradish peroxidase (HRP)-conjugated goat anti-rabbit IgG (H+L, Jackson ImmunoResearch Laboratories, Inc., West Grove, PA, USA), which was used at a dilution of 1:10,000 for detection of PLB, pPLB Ser-16, pPLB Thr-17 and pRyR Ser-2814, 1:20,000 for detection of RyR and pRyR Ser-2808, 1:60,000 for detection of GAPDH relative to PLB, 1:80 000 for detection of GAPDH relative to RyR and pRyR Ser-2808, and 1:100,000 for detection of GAPDH relative to pRyR Ser-2814.

Expression analysis. Expression was analysed as in Branovets et al. (2021) and Laasma et al. (2021), with the exception that the staining intensity was quantified using ImageJ. In short, the samples were distributed in random order on a gel, with each gel having two lanes allocated to the reference samples consisting of a mix of all samples for normalization. Each sample was measured at least two to three times in different gels. Before the measurements, dilutions of primary and secondary antibodies were calibrated to ensure the proportionality of

the measurement with the content of the protein of interest.

For the statistical analysis, the signal of the protein of interest was normalized to protein content or GAPDH intensity. For analysis of expression levels, all measurements were taken into account while linking all repeated measurements of each sample in the statistical software. When analysing phosphorylated state relative to overall expression of the protein, repeated measurements from each sample for the overall and phosphorylated state expressions were averaged before finding the ratio.

Statistics

If not stated otherwise, statistics are reported using means (SD). For independent measurements comparisons, we used unpaired Welch *t* test. For experiments repeated on several cells from the same animal, we used linear mixed models to study the impact of the fixed factors. In general, the models were composed with random intercepts. Where repeated measurements from the same cell were analysed (spark frequency at different amplitudes and t-tubular network length at different angles), the random intercepts were considered for nested random effects taking into account the animal–cell relationship. To determine significance of the fixed factor(s) and their interaction(s), the models with and without the corresponding factor or interaction were composed and *P*-values were obtained by likelihood ratio test of the full and simplified models. The models and comparisons used are described in Statistical Summary Document.

Statistical analysis was performed in R (R Core Team, 2023) using lme4 (Bates et al., 2015) for linear mixed models analysis. *P* < 0.05 was considered statistically significant.

Analysis was performed using scripts from IOCBIO Kinetics (Vendelin et al., 2020). Additional SQL and Python scripts were written to fetch the data from the database and used as an input for R statistical analysis scripts.

Results

Animals

The characteristics of the animals used in the study are given in Table 1. While age of the animals in the groups was not statistically different, males had a larger body weight, tibial length and heart weight. The heart weight to body weight ratio did not differ between males and females.

Ca²⁺ sparks are more frequent in females

When analysing Ca²⁺ spark measurements performed on cardiomyocytes from male and female mice, we observed

Table 1. Body weight, tibial length, and the heart weight of animals in different groups

Sex	Age (days) (n)	Body weight (g) (n)	Tibial length (cm) (n)	Heart weight (mg) (n)	Heart/body weight (n)
Female	255 ± 39 (28)	24.9 ± 2.5 (28)	2.20 ± 0.05 (28)	109 ± 22 (6)	4.3 ± 0.6 (6)
Male	275 ± 37 (22)	32.6 ± 3.6 (21)	2.26 ± 0.05 (22)	137 ± 6 (7)	4.3 ± 0.4 (6)
<i>P</i> (difference)	0.070	<0.001	<0.001	0.023	0.918

Data are shown as means ± SD (number of animals). Heart weight and the ratio of heart weight to body weight were only determined for the animals used for western blotting experiments. Values in bold indicate statistical significance.

that cardiomyocytes isolated from female mouse hearts had more sparks. Representative sparks (recorded raw trace, background corrected and pre-processed further before automatic sparks detection) are shown in Fig. 1A. The detected spark frequency depends on the amplitude of the detected spark event, as shown by the spark frequency distribution (Fig. 1B). As expected, the number of registered sparks was zero at small amplitudes, as these events are not detected by the algorithm (Laasmaa et al., 2019), and at very large amplitudes, as there are limits imposed by the junctional SR Ca²⁺ content available for release (Hou et al., 2023). When the cells were kept in the control solution, the difference in spark frequency distributions was non-significant. However, in the presence of ISO, we found that the mean spark frequency distribution had larger values in females compared to males (Fig. 1B). This is indicated by the statistically significant interaction between spark amplitude and sex (see statistical summary table at the right bottom of Fig. 1B).

As there were more Ca²⁺ sparks in the presence of ISO in female than in male cardiomyocytes, we analysed whether the sparks' duration and width depended on sex. For this analysis, we used sparks with amplitudes between 1.0 and 2.0 $\Delta F/F_0$. According to the statistical analysis of spark duration (Fig. 1C) and width (Fig. 1D), adrenergic stimulation increased spark width (Fig. 1D, effect of solution). However, sex and interaction between sex and solution were not statistically significant factors. Thus, in our experiments, we found overall that there was no difference in spark morphology between males and females.

To assess whether the difference in spark frequency between female and male cardiomyocytes was caused by differences in the number of highly active release sites, we analysed the frequency of spark pairs. If it was the case, we expected to observe a larger number of spark pairs per spark in the cells where active release sites dominate. For this analysis, we pooled all the recordings, found spark pairs as in Ramay et al. (2011), and analysed separately the measurements that had either at least two sparks (Fig. 1E) or at least one spark pair (Fig. 1F). We found a statistically significant difference when we used recordings that had at

least one spark pair in it (Fig. 1F). However, in this case, the significance was lost when we dropped a single recording from the dataset (largest value recorded for males), leading to $P = 0.107$. Thus, while the difference was observed for the full dataset, we prefer not to draw mechanistic conclusions from it.

The occurrence of waves was calculated for different time intervals after pacing and are shown in a cumulative wave count plot (Fig. 2). More waves occurred with time, as expected for a cumulative wave count from the moment the pacing was stopped. More waves were found in the presence of ISO, as indicated by the significant effect of solution and its interaction with time. Interestingly, despite the significantly higher spark frequency in female cardiomyocytes, their probability of exhibiting calcium waves was not different from that in male cardiomyocytes (Fig. 2).

Ca²⁺ transients are similar for females and males

As we found that the spark frequency was different in cardiomyocytes isolated from female and male mice in the presence of ISO, we looked into their Ca²⁺ transients (Fig. 3). In the presence of ISO, compared to the control solution, the Ca²⁺ transients had a shorter duration (Fig. 3B) and a larger amplitude (Fig. 3C), and the rates of rise and decay were significantly faster (Fig. 3D and E). According to our data, with the exception of an interaction between solution and sex in rise time, there was no effect of sex in the transient duration, amplitude, rate or time of rise, or decay (Fig. 3). Thus, both under control conditions and after β -adrenergic stimulation with ISO, the transients were similar in male and female cardiomyocytes.

Ca²⁺ transients have similar dyssynchrony index in females and males

We further studied the synchronicity of Ca²⁺ release and removal in cardiomyocytes using the same confocal line-scan images as in Fig. 3. For that, we found the time-moments before and after each Ca²⁺ transient peak, at which local F_{Ca} was at the half-maximal amplitude,

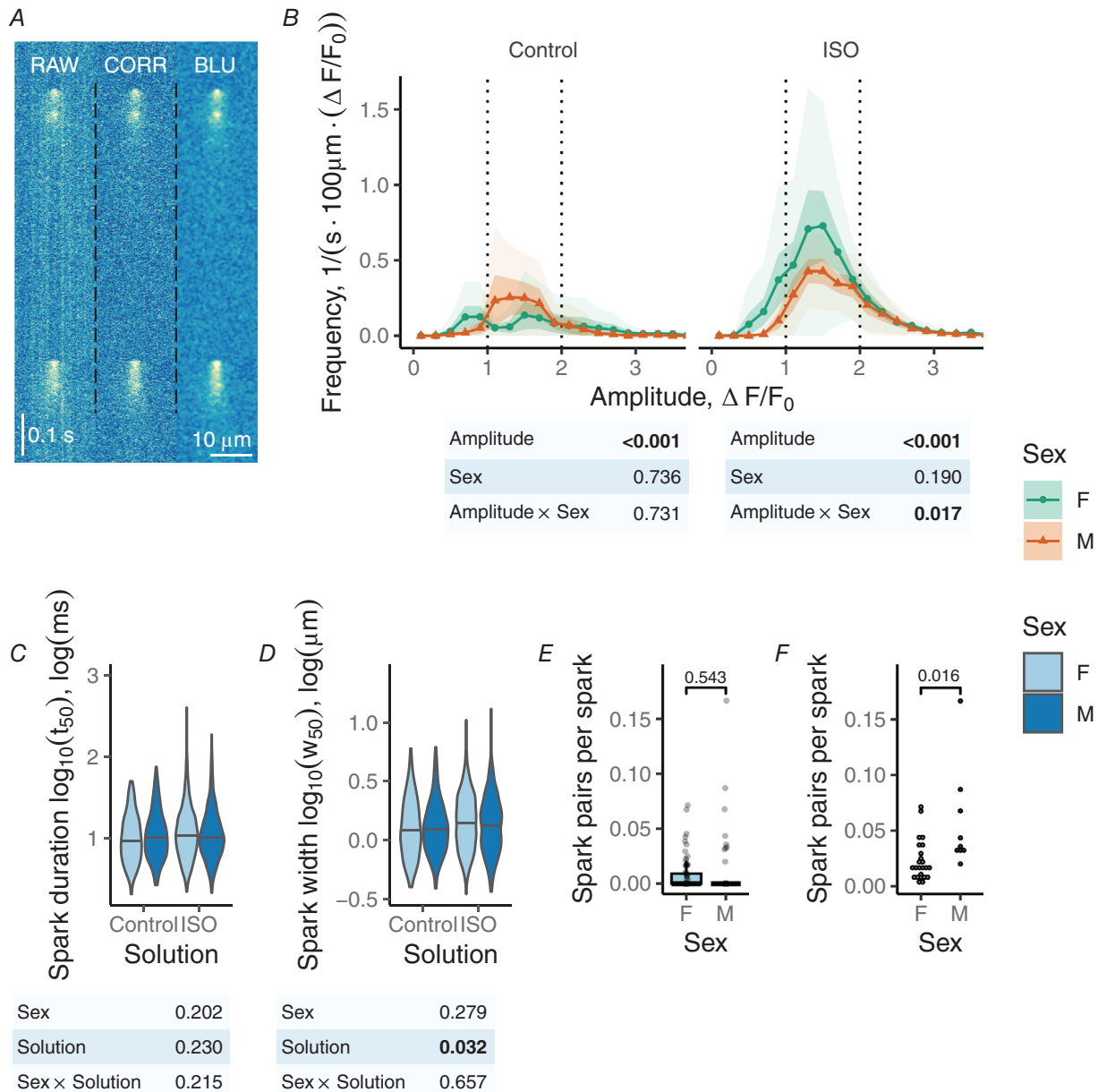


Figure 1. Sex influences Ca^{2+} sparks frequency and morphology

To summarize the subplots, a summary of statistical analysis by linear mixed models is depicted below the graphs and shows the significance of the factors. *A*, representative sparks measured in confocal microscope (RAW), with the corrected background (CORR) and after blurring (BLU) as done by the analysis software before spark detection and spark parameter estimation. *B*, mean spark frequency distribution (\pm SEM shown by darker shaded area; \pm SD shown as lighter shaded area) as a function of spark amplitude in the different groups. Here, the mean value was found by averaging data obtained on the animal first and then finding mean, SD and SEM from the animal-averaged dataset. Spark frequency was found to be significantly higher in females in ISO, as indicated by the significant interaction between spark amplitude and sex (the bottom panels showing significance of the factors). Vertical lines show the range of spark amplitudes used in the spark morphology analysis in *C* and *D*. *C* and *D*, spark duration (*C*, log₁₀ scale) and spark width (*D*, log₁₀ scale) were not influenced by sex, as shown in the bottom panels. *E* and *F*, number of spark pairs identified per spark among all experiments that have exhibited at least two sparks (*E*) or had at least one pair (*F*). Number of animals and cells used in the experiments were as follows (animals/cells): female (13/99), male (9/68). See statistical summary table for the results of all statistical tests. [Colour figure can be viewed at wileyonlinelibrary.com]

as shown in Fig. 4A. The statistical analysis of systolic (Fig. 4B) and diastolic (Fig. 4C) dyssynchrony indexes showed that, when the full dataset was analysed with linear mixed models, there was no statistically significant difference between sexes. For both sexes, Ca^{2+} release was more synchronous in the presence of ISO, which is indicated by the reduction of the systolic (Fig. 4B) and diastolic (Fig. 4C) dyssynchrony indexes. For the systolic dyssynchrony index, the difference between control and ISO was larger for males than females, which was reflected in an interaction between solution and sex. However, when comparing the indexes between sexes obtained for each solution separately, no statistically significant difference was found (Fig. 4).

Sex differences in longitudinal t-tubules

Modifications in the t-tubular network have previously been shown to relate to dyssynchronous Ca^{2+} release (Frisk et al., 2016; Kolstad et al., 2018; Louch et al.,

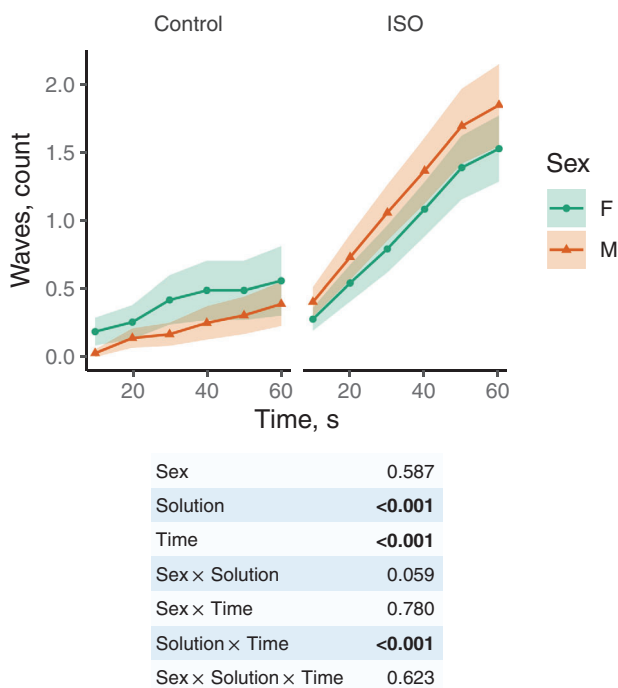


Figure 2. Ca^{2+} wave occurrence is not significantly different between female and male mouse cardiomyocytes

In the plot, the mean number of Ca^{2+} waves (\pm SEM) recorded after the final electrical stimulation of the cell is shown as a function of time elapsed after the last stimulation, i.e. as a cumulative wave count plot. A summary of the statistical analysis by linear mixed models is depicted below the graphs and shows the significance of the factors. Note that while there were more waves at the same time in the presence of ISO, the number of waves was similar for females and males. Number of animals and cells used in the experiments were as follows (animals/cells): female (13/115), male (9/88). [Colour figure can be viewed at wileyonlinelibrary.com]

2006). As shown in the representative images (Fig. 5A), we determined the location and orientation of all t-tubules on confocal images. When analysing the differences in overall length of the t-tubular network using linear mixed models, the difference between female and male was not statistically significant (Fig. 5B). The fractal dimension of the network, a measure describing how well the network is filling the space, was not statistically significantly different between sexes either (Fig. 5C). Next, we looked into how the t-tubules are oriented. For that, we partitioned all t-tubule sections according to their orientation using the same orientation angle ranges as used in the representative image (Fig. 5A). The length as a function of the orientation angle is shown in (Fig. 5D). As shown in the figure and indicated by the significance of angle and sex interaction (statistical analysis summary table at the bottom right of Fig. 5D), a difference between sexes was apparent in the longitudinal section. Namely, male compared to female cardiomyocytes had significantly more longitudinally oriented t-tubules when compared to the length at the diagonal section (marked '54–72°' in Fig. 5D). For a similar comparison in the transverse orientation, there was no statistically significant difference between the sexes. Thus, there are sex-differences in the longitudinally oriented t-tubules.

RyR clusters are larger in female than in male cardiomyocytes

Ca^{2+} transient synchrony, as well as spark properties, is affected by the distribution and size of RyR clusters. Therefore, we studied the RyR distribution in cardiomyocytes using dSTORM super-resolution imaging (Fig. 6). Representative images of RyRs from female and male mouse cardiomyocytes are shown in Fig. 6A and Supporting information Video S1 and demonstrate median RyR cluster sizes for both groups. From the analysis of the images, we found that, on average, female cardiomyocytes had 25% more RyRs in a cluster (Fig. 6B) than males. The same differences were also found in the number of RyRs per CRU (Fig. 6C), with RyR clusters assigned to the same CRU if the edges of the clusters were within 100 nm of each other (Sobie et al., 2006). The difference between sexes in number of clusters per CRU was not statistically significant (Fig. 6D). As we found significant differences in the number of RyRs in a single cluster and CRU, we looked at the average count of clusters and CRUs per unit volume (density) shown in Fig. 6F and G, respectively. For both parameters, we found that female mice had lower cluster and CRU density than males. The differences in cluster and CRU densities, however, were not caused by groups having a different level of RyR content. RyR content is reflected in overall RyR densities that were not different from each other for

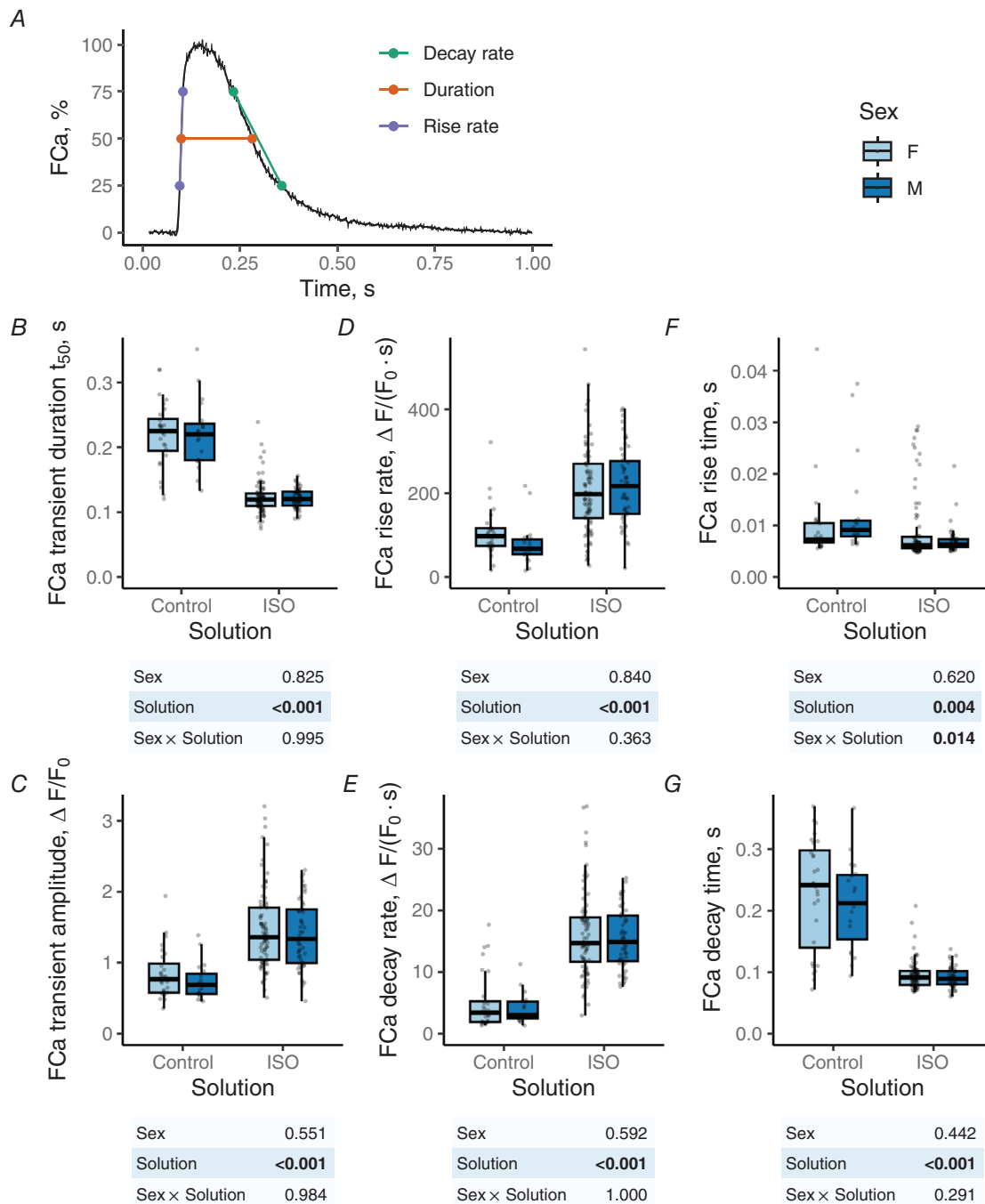


Figure 3. Ca^{2+} transients are not significantly different for cardiomyocytes from male and female mice

Ca^{2+} concentration changes were visualized using fluo-4 with its fluorescence F_{Ca} recorded by confocal microscope line-scan mode along a cardiomyocyte. Figure key is at the top right. To summarize the subplots, a summary of the statistical analysis by linear mixed models is depicted below the graphs and shows the significance of the factors. A, scheme visualizing determination of duration and rates of rise and decay for a transient. B and C, transient duration (B), measured at 50% of transient amplitude. In all cases, treatment with ISO reduced the duration statistically significantly. Transient amplitude (C) was significantly larger in ISO. D and E, rate of rise (D) and decay (E) were influenced only by solution, not sex. F and G, time of rise (F) and decay (G) were influenced only by solution. These times were found from delays between time points corresponding to 25% and 75% amplitude of the transient. Interaction between sex and solution was found to be significant for rise time (F), but sex was not a significant factor. Number of animals and cells used in the experiments were as follows (animals/cells): female (15/109), male (10/70). [Colour figure can be viewed at wileyonlinelibrary.com]

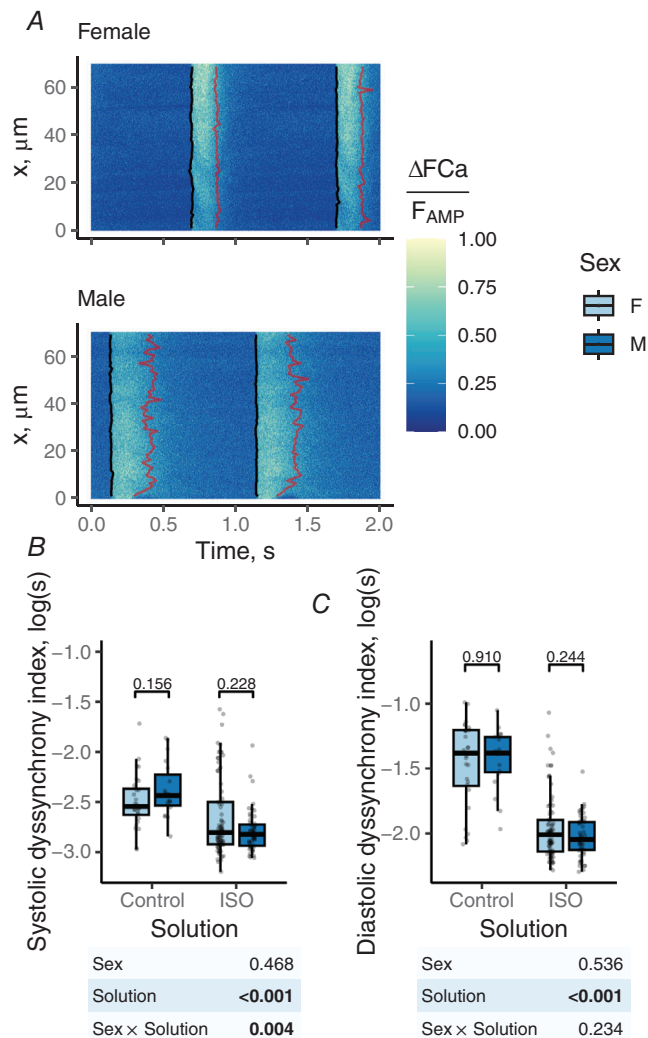


Figure 4. Dyssynchrony of calcium release is influenced by solution in healthy cardiomyocytes

The same raw data were analysed as in Fig 3. Figure key is on the top right. To summarize the subplots, a summary of the statistical analysis by linear mixed models is depicted below the graphs and shows the significance of the factors. A, representative examples showing Ca^{2+} release in female (top) and male (bottom) cardiomyocytes. The half-maximal amplitude before and after local fluorescence maxima are denoted by black and red lines, respectively. The variability of the detected lines in time was used to calculate the systolic and diastolic dyssynchrony index. B and C, the systolic (B) and diastolic (C) dyssynchrony index (larger value corresponds to larger dyssynchrony) for cardiomyocytes isolated from female and male mice. The index is shown on a logarithmic scale (base 10), with the larger value corresponding to a more dyssynchronous transient. In all cases, ISO treatment led to a more synchronous Ca^{2+} transient. For the systolic dyssynchrony index, the ISO effect was sex dependent as indicated by the statistical significance of sex and solution interaction. In each solution (Control and ISO), there was no statistically significant difference in the indexes between sexes. [Colour figure can be viewed at wileyonlinelibrary.com]

females and males (Fig. 6H). In summary, although the overall RyR density was the same and female compared to male cardiomyocytes had fewer and larger RyR clusters, resulting in a larger distance between CRUs in females.

No differences in the expression and phosphorylation of RyRs and PLB

As we found differences in spark frequency and organization of RyRs between sexes, we looked at the total expression of RyRs and their phosphorylation at Ser2808 and Ser2814, the protein kinase A (PKA) and Ca^{2+} /calmodulin-dependent protein kinase II (CaMKII) phosphorylation sites, respectively.

Representative images from the gels and the statistical analyses are shown in Fig. 7. We found no difference in the total expression of RyR (Fig. 7B) or its phosphorylated states. Phosphorylated RyR was analysed as total phosphorylated content (Fig. 7C and D) or related to overall expression (Fig. 7E and F). The similar total RyR expression (Fig. 7B) corroborates the RyR content estimated by dSTORM (Fig. 6H), where no differences were found either.

While we earlier did not find any statistically significant difference between sexes in L-type calcium channel (LTCC) and sarco/endoplasmic reticulum Ca^{2+} -ATPase (SERCA) expression (Laasmaa et al., 2021), we looked into the regulatory effect imposed by phospholamban, PLB and/or its phosphorylation on Ser16 (PKA phosphorylation) or Thr17 (CaMKII phosphorylation). We found that the expression of PLB and its phosphorylated forms was not statistically significantly different between sexes (Fig. 7G–I). Similar result was obtained for relative phosphorylation that was found to be not significantly different between sexes (Fig. 7J and K).

Results were confirmed by normalizing all measurements to GAPDH expression from the same samples (Supporting information, Fig. S1).

Discussion

In this study, we compared how basic Ca^{2+} handling relates to structural differences in female and male mouse cardiomyocytes. We found that, in female compared to male cardiomyocytes, the t-tubule network was shorter in the longitudinal direction, RyR clusters were larger and arranged differently while having similar RyR expression level, and Ca^{2+} spark frequency was higher. Intriguingly, despite these differences, the Ca^{2+} transients and the occurrence of Ca^{2+} waves were similar in male and female cardiomyocytes under control conditions as well as during β -adrenergic stimulation.

Differences in Ca^{2+} handling between female and male cardiomyocytes have been the subject of several studies.

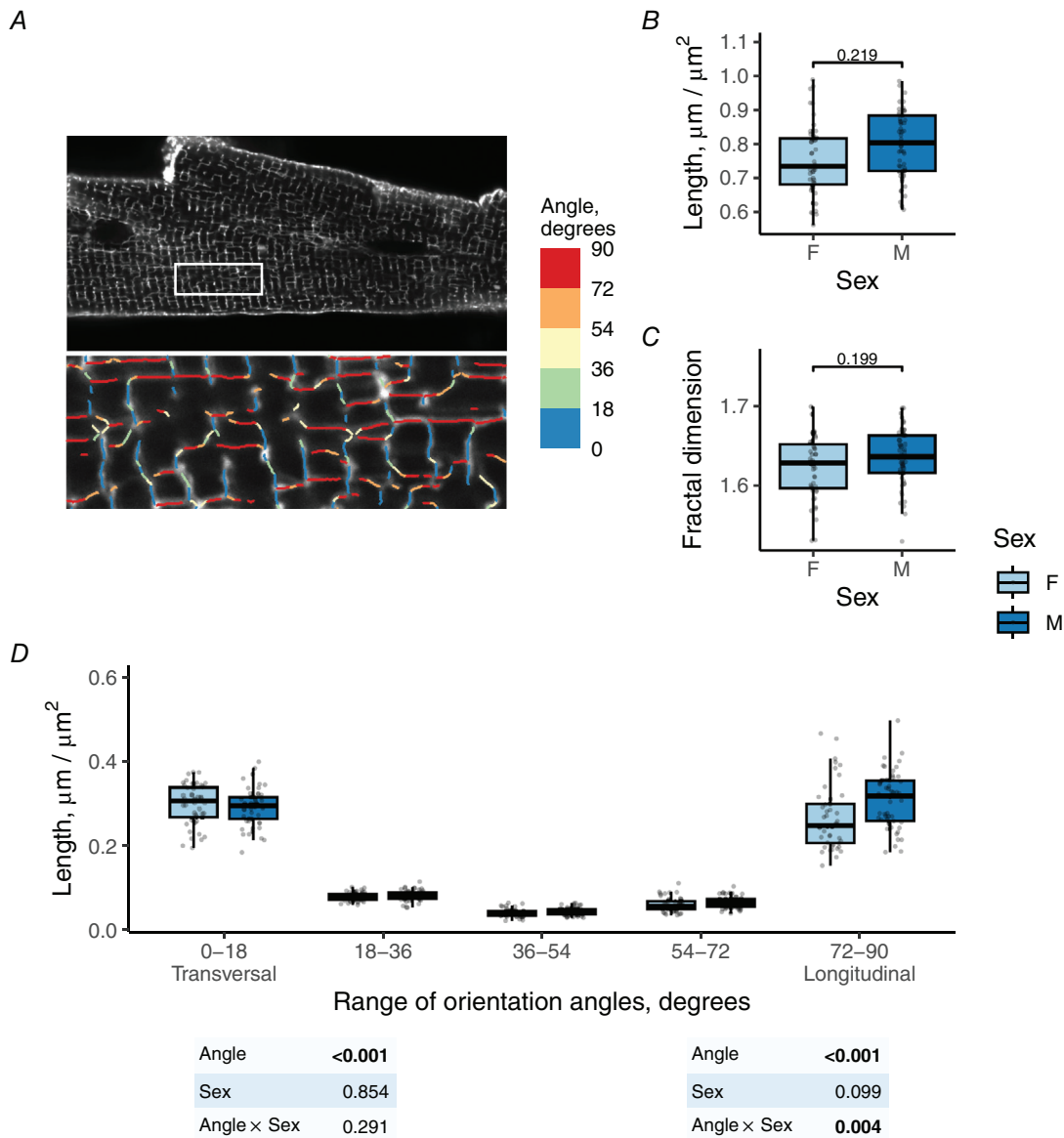


Figure 5. T-tubular network differences between sexes

Sarcolemma of live cardiomyocytes from female and male mice was labelled with CellMask and imaged with a confocal microscope. Figure key is on the right. *A*, representative images of the t-tubular network (top) in cardiomyocytes isolated from a male mouse. Here, individual confocal optical sections are shown. The automatic detection of the network in the small section of the image (section shown by white box $20 \times 7 \mu\text{m}$ on the image at the top) is demonstrated at the bottom. Orientation of t-tubules is divided into 5 groups from 0 to 90 degrees and indicated in colour, as shown on the right, with 0 degrees corresponding to the transverse orientation and 90 degrees to the longitudinal one. *B*, the overall length of the t-tubular network was not statistically significantly different when analysed by linear mixed models. Here, the length was normalized by the analysed area. *C*, fractal dimension, a measure of space-filling capacity, of the t-tubular network, was similar in males and females. *D*, the overall length of differently oriented segments of the t-tubular network clearly shows the more longitudinally oriented t-tubules in males than females. As shown in the statistical analysis tables below the plot, there is no statistical significance of sex nor interaction between sex and the orientation angle for t-tubular length oriented in transverse direction (angle groups used, 0–18 and 18–36 in the analysis, table on the left). In contrast, longitudinally oriented t-tubules have differences between sex as manifested by significant interaction between angle and sex (angle groups used, 54–72 and 72–90; table on the right). Number of animals and cells used in the experiments were as follows (animals/cells): female (5/47), male (5/53). [Colour figure can be viewed at wileyonlinelibrary.com]

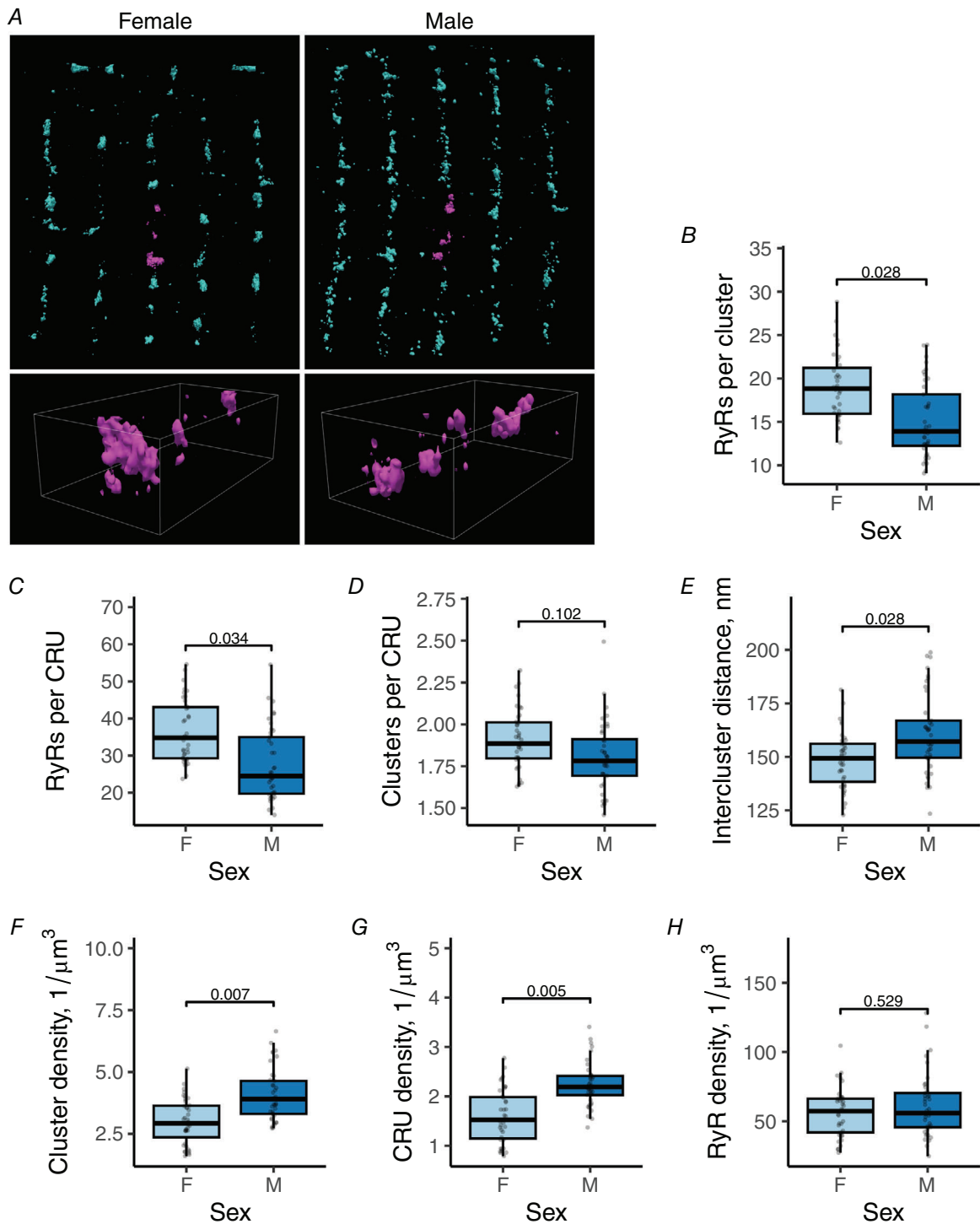


Figure 6. Analysis of super-resolution images of RyRs reveals multiple differences in the RyR organization of female and male littermates

A, representative images (top, $10 \times 12 \mu\text{m}$ image size) of RyRs in cardiomyocytes isolated from female and male mice. 3D rendering below shows RyR marked in magenta on the top image (box size $1.5 \times 2.55 \times 0.84 \mu\text{m}$). B–D, the number of RyRs in each cluster (B) and per CRU (C) was significantly higher in female than in male littermates, and sex differences in RyR clusters per CRU (D) were not statistically significant. E–G, the shortest distance between RyR clusters (E) was significantly smaller in cardiomyocytes from female than male mice; however, at the same time, the overall RyR cluster density (F), i.e. the number of clusters per volume, was smaller for females than for males, and CRU density (G) was higher in males than in females. H, the observed differences in RyR organization were

not the result of the difference in the overall RyR content, estimated via the number of RyRs per unit volume, RyR density. All the studied groups had a similar RyR density, and no statistically significant differences were found between the groups. Number of animals and cells used in the experiments were as follows (animals/cells): female (5/39), male (5/41). [Colour figure can be viewed at wileyonlinelibrary.com]

Most reviews describing sex differences in cardiomyocyte Ca^{2+} handling note that females, when compared to males, have smaller Ca^{2+} transients with lower Ca^{2+} spark amplitude and suggest that macroscopic sex difference in Ca^{2+} transients can be traced to the differences in Ca^{2+} release elementary events, lower excitation–contraction coupling gain and a smaller response to β -adrenergic stimulation (Parks et al., 2014; Prajapati et al., 2022; Regitz-Zagrosek & Kararigas, 2016). Taken together with the sex differences in the cAMP/PKA pathway, attenuation of SR Ca^{2+} release in females can explain those findings (Parks et al., 2014). However, as shown in Results and discussed below, our data do not fully agree with the proposed mechanism.

In part, it is possible to attribute the differences between our results and some earlier studies to the differences in the species, age and protocols used. There are some differences in the data recorded on rats compared to mice (see summary tables in review Prajapati et al., 2022). However, that only explains some of the differences from results reported in the literature.

Higher spark frequency in female cardiomyocytes can be explained by RyR cluster organization

In contrast to earlier studies on mice (Parks et al., 2014) and rats (Farrell et al., 2010; Yaras et al., 2007), we found that female cardiomyocytes had more sparks than male cardiomyocytes. Under control conditions, females tended to have more sparks, and in the presence of ISO, we found a clear statistically significant difference in spark frequency distribution (Fig. 1). When comparing the experiments performed in our study with the experiments in Farrell et al. (2010), Parks et al. (2014) and Yaras et al. (2007), we have used a protocol where sparks were measured right after a sequence of field stimulations. This allowed us to ensure that the cardiomyocytes contracted, as expected, before recording sparks. In our preparation, sparks were determined for a longer period (about 60 s or more) and analysed by newer software that has an improved background subtraction protocol and reduced false positive spark detection (Laasmaa et al., 2019). In Farrell et al. (2010) and Parks et al. (2014), based on the published methods, sparks seemed to be recorded for a short time (about 6 s) and cardiomyocyte function was not tested before the recordings. In the present experiments, the cardiomyocytes were paced at 1 Hz, and only contracting cells were selected for the experiments. The cells were contracting for at least 2 min before the start of the

experiments, so we are confident that our cell preparation was sound.

We did not include any analysis of average spark amplitude, as the estimation of the amplitude strongly depends on the spark's location with respect to the line scanned by the confocal microscope and other parameters (Izu et al., 1998). Instead, we analysed spark amplitude distributions (Fig. 1B). Based on this analysis, it is clear that females have more sparks over a large range of amplitudes when compared to males. Hence, our data do not suggest that females have smaller sparks.

To our knowledge, this is the first time sex differences in the RyR organization have been described. Here, we found that female RyR clusters are larger and located at larger distances from each other (Fig. 6). Similar to earlier studies (Parks et al., 2014), we found that total RyR expression, RyR Ser2808 and Ser2814 phosphorylation (PKA and CaMKII phosphorylation sites, respectively) did not differ between the sexes (Fig. 7B–F). The difference appears only in the RyR organization. As the RyR phosphorylation levels were the same in females and males, the difference in RyR arrangement could be related to sex hormones. Testosterone deficiency has been shown to significantly elevate RyR expression by ~1.5-fold in orchietomized male rats, whereas the administration of testosterone reverses this effect (Tsuneda et al., 2009). However, in the same study, the expression level of RyR between the female and male control groups is not statistically different, the same as our study. Despite this, there remains the possibility that the arrangement of RyRs differs due to testosterone, which requires further investigation.

It has been previously shown that the spark frequency correlates with the RyR cluster size (Galice et al., 2018). This is highly likely to be why we observed higher spark frequency in females than males, as we did not detect any changes in the phosphorylation state of RyRs between sexes, which could lead to the higher spark frequency (Shen et al., 2022). This phenomenon could be explained by the fact that a cluster with more RyRs increases the likelihood that the opening of one RyR will trigger the opening of others in the same cluster, leading to detectable sparks. Mathematical modelling supports this idea, showing that spark fidelity increases with more RyRs in a cluster, but below a certain cluster size, sparks are not detectable (Kolstad et al., 2018).

The frequency of Ca^{2+} waves in cardiomyocytes is linked to the frequency of Ca^{2+} sparks (Cheng & Lederer, 2008). While female cardiomyocytes had a higher spark frequency, our experiments showed that this did not

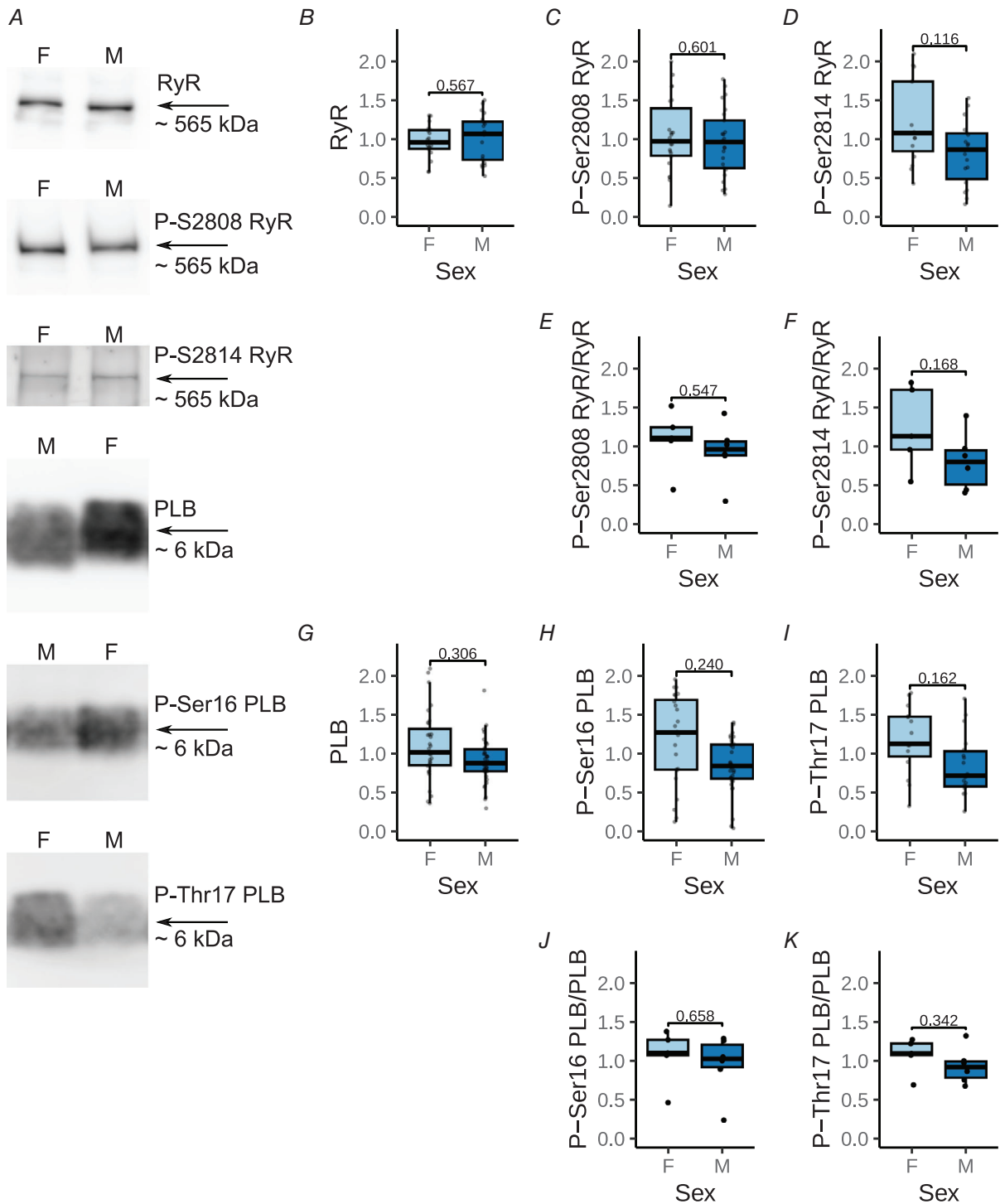


Figure 7. Data from western blot experiments to assess the expression and phosphorylation of RyR and PLB

Expression levels were related to the overall expression (male and female pooled together). A, Representative images from the gels. B–F, we found no differences between sexes in total RyR expression (B) or RyR phosphorylation using absolute (C and D) or relative to RyR expression (E and F) estimates. G–K, results of PLB expression and those of its phosphorylated forms. PLB expression and its phosphorylation states were not significantly different between sexes (G, H and I). In addition, relative phosphorylation was not significantly different (J and K). Five to six female and 6–7 male mice were used in the experiments. [Colour figure can be viewed at wileyonlinelibrary.com]

lead to a higher rate of Ca^{2+} waves (Fig. 2). In fact, the occurrence of waves was similar in both males and females, whether in control or the presence of ISO. This is likely because CRUs are further apart in females, making it more difficult for the spike in Ca^{2+} concentration caused by a spark to travel from one CRU to another and trigger additional Ca^{2+} release. As a result, local concentration changes are dampened more in cases of larger distances between CRUs before Ca^{2+} can reach a neighbouring CRU.

The other structural difference reported in our study is the organization of t-tubules (Fig. 5). The transverse t-tubules were similar in female and male cardiomyocytes, but there were more longitudinal t-tubules in males than in females. While changes in the t-tubular network have previously been shown to cause dyssynchronous Ca^{2+} release in heart failure (Frisk et al., 2016; Kolstad et al., 2018; Louch et al., 2006), this is associated with a decrease in the transverse t-tubules and an increase in longitudinal t-tubules (Lipsett et al., 2019). As there were no differences in the transverse t-tubules, where the dyadic space is formed between the sarcolemma and the SR, it is not surprising that the Ca^{2+} release dyssynchrony was very similar in female and male cardiomyocytes if we consider the spread of the estimated indexes (Fig. 4). However, such a difference in the t-tubular network between female and male cardiomyocytes in healthy cardiomyocytes could translate into larger differences in pathology, leading to a significant impact on cardiac function. Whether this is the case is a subject of further study.

Ca^{2+} transients and their response to ISO are similar in male and female cardiomyocytes

In our experiments, the Ca^{2+} transient characteristics, such as amplitude, duration and rate of rise or decay, did not differ between the sexes (Fig. 3). As shown in Fig. 3, the recorded data have a significant spread. However, the medians depicted on the graphs reflect the similarity of the traces recorded in females and males very well. Earlier studies have reported either larger Ca^{2+} transient amplitudes in males than in females (Curl et al., 2001; Farrell et al., 2010; Parks et al., 2014) or no statistical difference in amplitudes (Grandy & Howlett, 2006; Howlett, 2010). Similar inconclusiveness surrounds earlier reports on Ca^{2+} transient rise or decay rates, with some studies reporting slower rates for females than males (Curl et al., 2001; Farrell et al., 2010) and some showing no statistically significant difference (Farrell et al., 2010; Grandy & Howlett, 2006; Howlett, 2010). Unfortunately, the underlying spread of the data is not shown by individual recordings in the earlier reports. As a result, it is difficult to compare those datasets with our data.

According to our data, the Ca^{2+} handling of female and male cardiomyocytes responded similarly to β -adrenergic stimulation by ISO. This included the ISO impact on the Ca^{2+} transient (Fig. 3), dyssynchrony of Ca^{2+} release (Fig. 4), and Ca^{2+} sparks (Fig. 1). Remarkably, our data show no difference in ISO response in Ca^{2+} transients, as clearly indicated by the absence of any statistical significance of sex as a factor in the statistical analysis. Thus, our data are in contrast to earlier reports showing a dampened ISO response of female cardiomyocytes compared to males (Curl et al., 2001; Sun et al., 2006).

The influence of experimental protocol points to subtle sex differences that result in overall similar Ca^{2+} transients

In the present study, we used field stimulation to activate cardiomyocytes and record Ca^{2+} transients. This is similar to Curl et al. (2001) and Sun et al. (2006) and in contrast to other studies (Farrell et al., 2010; Grandy & Howlett, 2006; Howlett, 2010; Parks et al., 2014) where cardiomyocyte activation was performed with a microelectrode applying stimulation voltages vastly different from intrinsic action potentials. Earlier, as a part of our studies on the role of creatine kinase in the heart, we looked into Ca^{2+} channels and Ca^{2+} transients using patch clamp and applying square pulses to cardiomyocytes isolated from female and male mice (Laasmaa et al., 2021). In the current work context, for comparison with earlier electrophysiological studies on sex difference, we reanalysed the dataset from Laasmaa et al. (2021) using only wild-type mice. According to our earlier data on Ca^{2+} transients obtained using patch clamp stimulated cardiomyocytes, the Ca^{2+} transient amplitude was not statistically significantly different between female and male cardiomyocytes under control conditions. ISO treatment had a similar effect ($P < 0.0001$ for comparison between control and ISO for each of the sexes) on the Ca^{2+} transient amplitude, with no statistically significant difference observed between females and males and no statistically significant interaction between sex and ISO treatment (data reanalysed using mixed design ANOVA). However, the Ca^{2+} transient decay was longer in males than females under control conditions (t test, $P < 0.05$), and on the application of ISO, the decay was reduced more in males than females leading to a significant interaction between ISO and sex ($P < 0.001$). We did not find any sex differences in SERCA expression (Laasmaa et al., 2021) or PLB expression and phosphorylation (Fig. 7G–K), so that could not explain the slower Ca^{2+} transient decay in male cardiomyocytes.

We also analysed the LTCC current from our earlier study (Laasmaa et al., 2021). At the ion channel level, the maximal LTCC current was larger in females than in males ($P = 0.02$) under control conditions. This

result agrees with recordings in adult rabbits (Sims et al., 2008) and guinea pigs (Mason & MacLeod, 2009), and contrasts with the earlier recordings on mice and rats (Farrell et al., 2010; Grandy & Howlett, 2006; Howlett, 2010; Parks et al., 2014; Sun et al., 2006). According to our data, ISO increased the LTCC current ($P < 0.0001$), and there was a tendency for a larger increase of the maximal current in males than in females ($P = 0.055$), leading to similar maximal currents for both sexes in the presence of ISO. A larger effect of ISO on the LTCC current has been reported earlier in rats (Vizgirda et al., 2002), consistent with our observed tendency. In Vizgirda et al. (2002), while the LTCC current–voltage relationship did not show a statistically significant difference between sexes, mean current density was larger in females than in males under control conditions, in agreement with our data (Laasmaa et al., 2021). LTCC current decay, found in our earlier work (Laasmaa et al., 2021), was faster in females than in males ($P = 0.04$) under control conditions, with ISO reducing the decay similarly for both sexes (no statistically significant interactions between sex and ISO treatment when analysed by ANOVA). In other studies, no statistically significant difference in LTCC current decay was observed (Grandy & Howlett, 2006; Parks et al., 2014). SR content in the presence of ISO was not statistically significantly different between sexes, in agreement with Parks et al. (2014).

Thus, as the comparison between the present study and our earlier study (Laasmaa et al., 2021) demonstrates, the protocol of stimulation and solutions surrounding the cell can influence the results. In this case, the Ca^{2+} decay behaves differently when measured with the patch clamp protocol (which suggests some differences) or using field stimulation (no differences). Considering the non-physiological square pulse driving the membrane potential and multiple channel inhibitors used in patch clamp studies, we expect that the field-stimulated cardiomyocytes behave closer to the *in vivo* situation. As an alternative to field stimulation, action potential clamp techniques can be used, allowing assessment of the contribution of different Ca^{2+} currents under conditions close to *in vivo* (Laasmaa et al., 2016). Taken together, our results suggest subtle sex differences in the Ca^{2+} influx and efflux pathways and their response to ISO, but these differences are balanced, resulting in similar Ca^{2+} transients in male and female cardiomyocytes.

Limitations of the study

Sex differences in Ca^{2+} handling can be caused by differences in oestrogen and/or testosterone levels. The several effects of oestrogen and testosterone on the cardiac

calcium signalling machinery are well described in Tran (2020) and Ayaz & Howlett (2015), respectively.

The oestrogen levels in mice can be affected by phytoestrogens in the food. Phytoestrogens are naturally occurring compounds in plants, which bind to oestrogen receptors and exert estrogenic or antioestrogenic effects (Dixon, 2004). In the present study, the mice received standard rat/mouse maintenance chow from Ssniff (R/M-H; Ssniff Spezialdiäten GmbH). It contains soybean, which has high levels of the isoflavones genistein and daidzein (Dixon, 2004), and the phytoestrogen content of this chow is indeed relatively high (Jensen & Ritskes-Hoitinga, 2007). However, as male and female mice received the same diet, the phytoestrogen content cannot cancel out the sex differences.

Summary

Summarizing our data in this work and our earlier patch clamp measurements (Laasmaa et al., 2021), we can reproduce the larger β -adrenergic response in males compared to females only in terms of the LTCC current properties and Ca^{2+} transient decay in the patch clamp set-up. As for Ca^{2+} dynamics recorded using field-stimulated cardiomyocytes, including transients and sparks, our data do not point towards a sex-dependent ISO effect, nor are they consistent with the hypothesis uniting smaller Ca^{2+} sparks, smaller Ca^{2+} transients and reduced ISO response in females compared to males. According to our data, Ca^{2+} sparks were more frequent in female than male cardiomyocytes, but that did not translate into differences in the Ca^{2+} transients, and female and male cardiomyocytes responded to β -adrenergic stimulation in a similar way. We identified differences between female and male cardiomyocytes in the organization of RyRs and the t-tubular network – structures playing a central role in Ca^{2+} handling. As we found no differences in the overall RyR expression and phosphorylation, our data suggest that the higher spark frequency in female cardiomyocytes relates to the organization of RyRs into larger, but fewer clusters.

References

- Allan, C., Burel, J. M., Moore, J., Blackburn, C., Linkert, M., Loynton, S., Macdonald, D., Moore, W. J., Neves, C., Patterson, A., Porter, M., Tarkowska, A., Loranger, B., Avondo, J., Lagerstedt, I., Lianas, L., Leo, S., Hands, K., Hay, R. T., ... Swedlow, J. R. (2012). OMERO: Flexible, model-driven data management for experimental biology. *Nature Methods*, **9**(3), 245–253.
- Ayaz, O., & Howlett, S. E. (2015). Testosterone modulates cardiac contraction and calcium homeostasis: Cellular and molecular mechanisms. *Biology of Sex Differences*, **6**(1), 9.

- Baddeley, D., Cannell, M. B., & Soeller, C. (2011). Three-dimensional sub-100 nm super-resolution imaging of biological samples using a phase ramp in the objective pupil. *Nano Research*, **4**(6), 589–598.
- Bates, D., Mächler, M., Bolker, B., & Walker, S. (2015). Fitting linear mixed-effects models using lme4. *Journal of Statistical Software*, **67**(1), 1–48.
- Beale, A. L., Meyer, P., Marwick, T. H., Lam, C. S. P., & Kaye, D. M. (2018). Sex differences in cardiovascular pathophysiology. *Circulation*, **138**(2), 198–205.
- Berg, S., Kutra, D., Kroeger, T., Straehle, C. N., Kausler, B. X., Haubold, C., Schiegg, M., Ales, J., Beier, T., Rudy, M., Eren, K., Cervantes, J. I., Xu, B., Beuttenmueller, F., Wolny, A., Zhang, C., Koethe, U., Hamprecht, F. A., & Kreshuk, A. (2019). ilastik: Interactive machine learning for (bio)image analysis. *Nature Methods*, **16**(12), 1226–1232.
- Branovets, J., Karro, N., Barsunova, K., Laasmaa, M., Lygate, C. A., Vendelin, M., & Birkedal, R. (2021). Cardiac expression and location of hexokinase changes in a mouse model of pure creatine deficiency. *American Journal of Physiology. Heart and Circulatory Physiology*, **320**(2), H613–H629.
- Branovets, J., Sepp, M., Kotlyarova, S., Jepihhina, N., Sokolova, N., Aksentijevic, D., Lygate, C. A., Neubauer, S., Vendelin, M., & Birkedal, R. (2013). Unchanged mitochondrial organization and compartmentation of high-energy phosphates in creatine deficient GAMT^{-/-} mouse heart. *American Journal of Physiology. Heart and Circulatory Physiology*, **305**(4), H506–H520.
- Cheng, H., & Lederer, W. J. (2008). Calcium Sparks. *Physiological Reviews*, **88**(4), 1491–1545.
- Choe, C., Nabuurs, C., Stockebrand, M. C., Neu, A., Nunes, P., Morellini, F., Sauter, K., Schillemeit, S., Hermans-Borgmeyer, I., Marescau, B., Heerschap, A., & Isbrandt, D. (2013). l-arginine:glycine amidinotransferase deficiency protects from metabolic syndrome. *Human Molecular Genetics*, **22**(1), 110–123.
- Curl, C. L., Wendt, I. R., & Kotsanas, G. (2001). Effects of gender on intracellular [Ca²⁺] in rat cardiac myocytes. *Pflugers Archiv: European Journal of Physiology*, **441**(5), 709–716.
- Dixon, R. A. (2004). Phytoestrogens. *Annual Review of Plant Biology*, **55**(1), 225–261.
- Farrell, S. R., Ross, J. L., & Howlett, S. E. (2010). Sex differences in mechanisms of cardiac excitation-contraction coupling in rat ventricular myocytes. *American Journal of Physiology. Heart and Circulatory Physiology*, **299**(1), H36–H45.
- Frisk, M., Ruud, M., Espe, E. K. S., Aronsen, J. M., Røe, Å. T., Zhang, L., Norseng, P. A., Sejersted, O. M., Christensen, G. A., Sjaastad, I., & Louch, W. E. (2016). Elevated ventricular wall stress disrupts cardiomyocyte t-tubule structure and calcium homeostasis. *Cardiovascular Research*, **112**(1), 443–451.
- Galice, S., Xie, Y., Yang, Y., Sato, D., & Bers, D. M. (2018). Size matters: Ryanodine receptor cluster size affects arrhythmogenic sarcoplasmic reticulum calcium release. *Journal of the American Heart Association: Cardiovascular and Cerebrovascular Disease*, **7**(13), e008724.
- Grandy, S. A., & Howlett, S. E. (2006). Cardiac excitation-contraction coupling is altered in myocytes from aged male mice but not in cells from aged female mice. *American Journal of Physiology. Heart and Circulatory Physiology*, **291**(5), H2362–H2370.
- Hou, Y., Laasmaa, M., Li, J., Shen, X., Manfra, O., Nordén, E. S., Le, C., Zhang, L., Sjaastad, I., Jones, P. P., Soeller, C., & Louch, W. E. (2023). Live-cell photoactivated localization microscopy correlates nanoscale ryanodine receptor configuration to calcium sparks in cardiomyocytes. *Nature Cardiovascular Research*, **2**(3), 251–267.
- Howlett, S. E. (2010). Age-associated changes in excitation-contraction coupling are more prominent in ventricular myocytes from male rats than in myocytes from female rats. *American Journal of Physiology. Heart and Circulatory Physiology*, **298**(2), H659–H670.
- Izu, L. T., Gil Wier, W., & William Balke, C. (1998). Theoretical analysis of the Ca²⁺ spark amplitude distribution. *Biophysical Journal*, **75**(3), 1144–1162.
- Jensen, M. N., & Ritskes-Hoitinga, M. (2007). How isoflavone levels in common rodent diets can interfere with the value of animal models and with experimental results. *Laboratory Animals*, **41**(1), 1–18.
- Keller, K. M., & Howlett, S. E. (2016). Sex differences in the biology and pathology of the aging heart. *Canadian Journal of Cardiology*, **32**(9), 1065–1073.
- Kolstad, T. R., van den Brink, J., MacQuaide, N., Lunde, P. K., Frisk, M., Aronsen, J. M., Norden, E. S., Cataliotti, A., Sjaastad, I., Sejersted, O. M., Edwards, A. G., Lines, G. T., & Louch, W. E. (2018). Ryanodine receptor dispersion disrupts Ca²⁺ release in failing cardiac myocytes. *eLife*, **7**, e39427.
- Laasmaa, M., Birkedal, R., & Vendelin, M. (2016). Revealing calcium fluxes by analyzing inhibition dynamics in action potential clamp. *Journal of Molecular and Cellular Cardiology*, **100**, 93–108.
- Laasmaa, M., Branovets, J., Barsunova, K., Karro, N., Lygate, C. A., Birkedal, R., & Vendelin, M. (2021). Altered calcium handling in cardiomyocytes from arginine-glycine amidinotransferase-knockout mice is rescued by creatine. *American Journal of Physiology. Heart and Circulatory Physiology*, **320**(2), H805–H825.
- Laasmaa, M., Karro, N., Birkedal, R., & Vendelin, M. (2019). IOCBIO Sparks detection and analysis software. *PeerJ*, **7**, e6652.
- Lipsett, D. B., Frisk, M., Aronsen, J. M., Nordén, E. S., Buonarati, O. R., Cataliotti, A., Hell, J. W., Sjaastad, I., Christensen, G., & Louch, W. E. (2019). Cardiomyocyte substructure reverts to an immature phenotype during heart failure. *The Journal of Physiology*, **597**(7), 1833–1853.
- Louch, W. E., Mørk, H. K., Sexton, J., Strømme, T. A., Laake, P., Sjaastad, I., & Sejersted, O. M. (2006). T-tubule disorganization and reduced synchrony of Ca²⁺ release in murine cardiomyocytes following myocardial infarction. *The Journal of Physiology*, **574**(2),

- 519–533.
- Mason, S. A., & MacLeod, K. T. (2009). Cardiac action potential duration and calcium regulation in males and females. *Biochemical and Biophysical Research Communications*, **388**(3), 565–570.
- Odening, K. E., Deiß, S., Dilling-Boer, D., Didenko, M., Eriksson, U., Nedios, S., Ng, F. S., Roca Luque, I., Sanchez Borque, P., Vernooy, K., Wijnmaalen, A. P., & Yorgun, H. (2019). Mechanisms of sex differences in atrial fibrillation: Role of hormones and differences in electrophysiology, structure, function, and remodelling. *European Pharmacopoeia*, **21**(3), 366–376.
- Olivier, N., Keller, D., Rajan, V. S., Gönczy, P., & Manley, S. (2013). Simple buffers for 3D STORM microscopy. *Biomedical Optics Express*, **4**(6), 885–899.
- Parks, R. J., & Howlett, S. E. (2013). Sex differences in mechanisms of cardiac excitation–contraction coupling. *Pflugers Archiv: European Journal of Physiology*, **465**(5), 747–763.
- Parks, R. J., Ray, G., Bienvenu, L. A., Rose, R. A., & Howlett, S. E. (2014). Sex differences in SR Ca²⁺ release in murine ventricular myocytes are regulated by the cAMP/PKA pathway. *Journal of Molecular and Cellular Cardiology*, **75**, 162–173.
- Prajapati, C., Koivumäki, J., Pekkanen-Mattila, M., & Aalto-Setälä, K. (2022). Sex differences in heart: From basics to clinics. *European Journal of Medical Research*, **27**(1), 241.
- R Core Team (2023). R: A Language and Environment for Statistical Computing. Advance online publication. <https://www.R-project.org>.
- Ramay, H. R., Liu, O. Z., & Sobie, E. A. (2011). Recovery of cardiac calcium release is controlled by sarcoplasmic reticulum refilling and ryanodine receptor sensitivity. *Cardiovascular Research*, **91**(4), 598–605.
- Regitz-Zagrosek, V., & Kararigas, G. (2016). Mechanistic pathways of sex differences in cardiovascular disease. *Physiological Reviews*, **97**(1), 1–37.
- Schmidt, A., Marescau, B., Boehm, E. A., Renema, W. K., Peco, R., Das, A., Steinfeld, R., Chan, S., Wallis, J., Davidoff, M., Ullrich, K., Waldschutz, R., Heerschap, A., De Deyn, P. P., Neubauer, S., & Isbrandt, D. (2004). Severely altered guanidino compound levels, disturbed body weight homeostasis and impaired fertility in a mouse model of guanidinoacetate N-methyltransferase (GAMT) deficiency. *Human Molecular Genetics*, **13**(9), 905–921.
- Shen, X., van den Brink, J., Bergan-Dahl, A., Kolstad, T. R., Norden, E. S., Hou, Y., Laasmaa, M., Aguilar-Sanchez, Y., Quick, A. P., Espe, E. K., Sjaastad, I., Wehrens, X. H., Edwards, A. G., Soeller, C., & Louch, W. E. (2022). Prolonged β -adrenergic stimulation disperses ryanodine receptor clusters in cardiomyocytes and has implications for heart failure ed. Huang CL-H & Aldrich RW. *eLife*, **11**, e77725.
- Sims, C., Reisenweber, S., Viswanathan, P. C., Choi, B.-R., Walker, W. H., & Salama, G. (2008). Sex, age, and regional differences in L-type calcium current are important determinants of arrhythmia phenotype in rabbit hearts with drug-induced long QT Type 2. *Circulation Research*, **102**(9), e86–e100.
- Sobie, E. A., Guatimosim, S., Gómez-Viquez, L., Song, L.-S., Hartmann, H., Saleet Jafri, M., & Lederer, W. J. (2006). The Ca²⁺ leak paradox and “rogue ryanodine receptors”: SR Ca²⁺ efflux theory and practice. *Progress in Biophysics and Molecular Biology*, **90**(1–3), 172–185.
- St Pierre, S. R., Peirlinck, M., & Kuhl, E. (2022). Sex matters: A comprehensive comparison of female and male hearts. *Frontiers in Physiology*, **13**, 831179.
- Sun, J., Picht, E., Ginsburg, K. S., Bers, D. M., Steenbergen, C., & Murphy, E. (2006). Hypercontractile female hearts exhibit increased S-nitrosylation of the L-Type Ca²⁺ channel α 1 subunit and reduced ischemia/reperfusion injury. *Circulation Research*, **98**(3), 403–411.
- Tran, Q.-K. (2020). Reciprocity between estrogen biology and calcium signaling in the cardiovascular system. *Frontiers in Endocrinology*, **11**, 568203.
- Trexler, C. L., Odell, A. T., Jeong, M. Y., Dowell, R. D., & Leinwand, L. A. (2017). Transcriptome and functional profile of cardiac myocytes is influenced by biological sex. *Circulation-Cardiovascular Genetics*, **10**(5), e001770.
- Tsuneda, T., Yamashita, T., Kato, T., Sekiguchi, A., Sagara, K., Sawada, H., Aizawa, T., Fu, L.-T., Fujiki, A., & Inoue, H. (2009). Deficiency of testosterone associates with the substrate of atrial fibrillation in the rat model. *Journal of Cardiovascular Electrophysiology*, **20**(9), 1055–1060.
- Vendelin, M., Laasmaa, M., Kalda, M., Branovets, J., Karro, N., Barsunova, K., & Birkedal, R. (2020). IOC BIO Kinetics: An open-source software solution for analysis of data traces. *PLoS Computational Biology*, **16**(12), e1008475.
- Vizgirda, V. M., Wahler, G. M., Sondgeroth, K. L., Ziolo, M. T., & Schwertz, D. W. (2002). Mechanisms of sex differences in rat cardiac myocyte response to β -adrenergic stimulation. *American Journal of Physiology. Heart and Circulatory Physiology*, **282**(1), H256–H263.
- Walker, C. J., Schroeder, M. E., Aguado, B. A., Anseth, K. S., & Leinwand, L. A. (2021). Matters of the heart: Cellular sex differences. *Journal of Molecular and Cellular Cardiology*, **160**, 42–55.
- Walt van der, S., Schönberger, J. L., Nunez-Iglesias, J., Boulogne, F., Warner, J. D., Yager, N., Gouillart, E., & Yu, T. (2014). scikit-image: Image processing in Python. *PeerJ*, **2**, e453.
- Wang, A., Yan, X., & Wei, Z. (2018). ImagePy: an open-source, Python-based and platform-independent software package for bioimage analysis. *Bioinformatics*, **34**(18), 3238–3240.
- Yaras, N., Tuncay, E., Purali, N., Sahinoglu, B., Vassort, G., & Turan, B. (2007). Sex-related effects on diabetes-induced alterations in calcium release in the rat heart. *American Journal of Physiology. Heart and Circulatory Physiology*, **293**(6), H3584–H3592.
- Yusifov, A., Chhatre, V. E., Zumo, J. M., Cook, R. F., McNair, B. D., Schmitt, E. E., Woulfe, K. C., & Bruns, D. R. (2021). Cardiac response to adrenergic stress differs by sex and across the lifespan. *GeroScience*, **43**(4), 1799–1813.
- Yusifov, A., Woulfe, K. C., & Bruns, D. R. (2022). Mechanisms and implications of sex differences in cardiac aging. *The Journal of Cardiovascular Aging*, **2**, 20.

Additional information

Data availability statement

All data supporting the results are included in the figures or, for larger datasets, as Supporting information. The datasets generated during and/or analysed during the current study are available from the corresponding author upon reasonable request. Analysis tools used are referred to in Methods either through references or, in the newly developed code, through open source software repository link.

Competing interests

The authors declares that they have no competing interests.

Author contributions

M.L., X.S.: superresolution imaging; J.B.: Ca²⁺ transients and sparks measurements and primary data analysis, t-tubular network imaging; M.L.: RyR clusters morphology analysis, Ca²⁺ waves detection from the data; M.V.: design of t-tubular network morphology detection algorithm; C.G., E.H.: t-tubular detection neural network training and optimization; J.S., T.R., M.J.B.: western blotting; R.B., J.B.: animal management, genotyping, isolation of cardiomyocytes; M.V.: data analysis and statistics; M.V., R.B., M.L.: conceptualized the project; M.V., R.B., W.E.L.: supervised the project; M.V.: drafted the manuscript; M.L., R.B.: edited the manuscript; all authors revised manuscript critically for important intellectual content. All authors have read and approved the final version of this manuscript and agree to be accountable for all aspects of the work in ensuring that questions

related to the accuracy or integrity of any part of the work are appropriately investigated and resolved. All persons designated as authors qualify for authorship, and all those who qualify for authorship are listed.

Funding

This work was supported by the Estonian Research Council (PRG1127).

Keywords

calcium dynamics, excitation–contraction coupling, heart, sex differences

Supporting information

Additional supporting information can be found online in the Supporting Information section at the end of the HTML view of the article. Supporting information files available:

Statistical summary document

Peer Review History

Supporting Figure S1

Supporting Video S1

Supporting Raw Data